

## THE EFFECT OF LOW EARTH ORBIT EXPOSURE ON SOME EXPERIMENTAL FLUORINE AND SILICON-CONTAINING POLYMERS

John W. Connell<sup>1</sup>, Philip R. Young<sup>1</sup>, Carol G. Kalil<sup>2</sup>, Alice C. Chang<sup>3</sup> and Emilie J. Siochi<sup>3</sup>

<sup>1</sup>NASA Langley Research Center

Hampton, VA 23681-0001

<sup>2</sup>Analytical Services and Materials

Hampton, VA 23666

<sup>3</sup>Lockheed Engineering and Sciences

Hampton, VA 23666

### ABSTRACT

Several experimental fluorine and silicon-containing polymers in film form were exposed to low Earth orbit (LEO) on a Space Shuttle flight experiment (STS- 46, Evaluation of Oxygen Interaction with Materials, EOIM-III). The environmental parameters of primary concern were atomic oxygen (AO) and ultraviolet (UV) radiation. The materials were exposed to  $2.3 \pm 0.1 \times 10^{20}$  oxygen atoms/cm<sup>2</sup> and 30.6 UV sun hours during the flight. In some cases, the samples were exposed at ambient, 120°C and 200°C. The effects of exposure on these materials were assessed utilizing a variety of characterization techniques including optical, scanning electron (SEM) and scanning tunneling (STM) microscopy, UV-visible (UV-VIS) transmission, diffuse reflectance infrared (DR-FTIR), x-ray photoelectron (XPS) spectroscopy and, in a few cases, gel permeation chromatography (GPC). In addition, weight losses of the films, presumably due to AO erosion, were measured. The fluorine-containing polymers exhibited significant AO erosion and exposed films were diffuse or "frosted" in appearance and consequently displayed dramatic reductions in optical transmission. The silicon-containing films exhibited minimum AO erosion and the optical transmission of exposed films was essentially unchanged. The silicon near the exposed surface in the films was converted to silicate/silicon oxide upon AO exposure which subsequently provided protection for the underlying material. The silicon-containing epoxies are potentially useful as AO resistant coatings and matrix resins as they are readily processed into carbon fiber reinforced composites and cured via electron radiation.

### INTRODUCTION

Evaluation of Oxygen Interactions with Materials-III (EOIM-III) is the third in a continuing series of materials exposure experiments flown aboard the space shuttle. This particular experiment was flown in August 1992 aboard Atlantis (STS-46). The primary parameters of concern for organic polymeric materials aboard EOIM-III were atomic oxygen (AO) and ultraviolet (UV) radiation. Other parameters that can

affect organic polymeric materials such as vacuum, thermal cycling, particulate radiation, and micrometeoroids and debris are less important for short term low Earth orbit (LEO) space flight experiments. The materials in this flight experiment were exposed to  $2.3 \pm 0.1 \times 10^{20}$  oxygen atoms/cm<sup>2</sup> and 30.6 ultraviolet sun hours. Some of the samples were also exposed at different temperatures (ambient, 120° and 200°C). AO is known from previous space flight experiments, of both short and long duration, to cause substantial erosion and mass loss of organic polymers<sup>1-4</sup>. Certain perfluorinated polymers, such as copolytetrafluoroethylene have exhibited good resistance to AO in both ground based and space flight exposure experiments. However, simultaneous exposure to AO and UV radiation can dramatically increase the rate of degradation of this material<sup>5,6</sup>. Coatings of inorganic oxides such as aluminum oxide<sup>7</sup>, silicon oxide<sup>7</sup>, chromium oxide<sup>8</sup> and indium-tin oxide<sup>9</sup>, as well as decaborane-containing polymers<sup>10</sup>, have been shown to protect organic materials from oxygen plasma and/or AO erosion. To provide maximum protection, the coatings need to be ~500-2000 Å thick, relatively uniform and defect free.

High performance polymers, such as polyimides, have been modified by the incorporation of silicon in the form of siloxane groups, either in the polymer backbone or pendant on the polymer chain. In addition to other favorable effects, the incorporation of silicon-containing groups into these polymers has been observed to enhance oxygen plasma/AO resistance through the formation of inorganic silicon (i.e. silicates/silicon dioxide) species by interacting with AO or oxygen plasma.<sup>3,5,11-17</sup> Other polymers containing silicon, such as poly(carborane siloxane)s, have also exhibited excellent oxygen plasma resistance.<sup>18</sup>

UV radiation present in LEO is of sufficient energy to cause organic bond cleavage. Organic polymeric materials can undergo UV induced chain scission and crosslinking reactions resulting in darkening, thermal conductivity, optical and mechanical property changes, embrittlement and loss of strength. These material property changes can dramatically affect spacecraft performance and lifetime.

Many of the experimental polymers flown on this experiment had shown promise in regards to AO and/or UV resistance in ground based exposure experiments. Low color, fluorinated polyimides<sup>19</sup> have been shown to be relatively resistant to electron and UV radiation in ground based experiments. Fluorine-containing poly(arylene ether)s had been shown to be resistant to electron radiation<sup>20</sup>. The silicon-containing materials had exhibited lower weight loss rates than Kapton®HN when exposed to oxygen plasma.<sup>15,16</sup> The intent of the work described herein was to increase our understanding of space environmental effects on fluorine and silicon-containing high performance polymers to aid in the design of future, lightweight materials with improved space environmental durability. The results of LEO exposure on these materials are discussed and, where relevant, compared to results from ground based exposures.

## EXPERIMENTAL

### Fluorine-Containing Polymers

The fluorine-containing polyimides<sup>21</sup> were prepared using the following general procedure. Stoichiometric quantities of the appropriate diamine and dianhydride were placed in N,N-dimethylacetamide (15-20% solids). The resulting solution was stirred at room temperature under nitrogen for 16-24 hr to form a viscous poly(amide acid) solution. This solution was subsequently cast onto plate glass and placed in a flowing dry air chamber until the film was tack-free. The tack-free film was placed in a forced air oven and heated for 1 hr each at 100, 200 and 300°C to effect imidization and solvent removal. The film was removed from the glass and characterized. The fluorine-containing poly(arylene ether)<sup>22</sup> and the copoly(imide-arylene ether)<sup>23</sup> were prepared as previously reported. The chemical structures of the fluorine-containing polymers are presented in Figure 1.

### Silicon-Containing Polymers

The epoxy functionalized siloxanes (EFS) were synthesized and cured using a UV source as previously described.<sup>24</sup> The polyimide containing pendent siloxane groups was prepared as previously reported.<sup>15</sup> The chemical structures of the silicon-containing polymers are presented in Figure 2.

Thin films (0.001-0.003 in. thick) were prepared and characterized prior to integration onto the EOIM-III experimental platform. Both control and flight experiment specimens were taken from the same piece of film. It should be noted that some of the flight specimens were exposed at elevated temperatures while the controls were stored under ambient conditions and did not receive additional thermal treatment. The characterization data determined on the flight specimens presented herein is relative to that of the control specimens which had been stored on Earth for ~2 years.

### Characterization

Ultraviolet-visible (UV-VIS) transmission spectra were recorded on a Perkin-Elmer Lambda 5 spectrometer. Infrared spectra were obtained by diffuse reflectance on a Nicolet Magna-IR System 750 spectrometer (DR-FTIR). Scanning tunneling microscopy (STM) was performed in air on a Nanoscope II instrument (Digital Instrument, Inc., Santa Barbara, CA) using a tungsten tip and G-Head accessory. Specimens were prepared by coating with a 5-8 nm of gold-palladium using a Hummer IV sputtering system (Anatech, Ltd., Alexandria, VA). A Cambridge Stereoscan 240 (Cambridge Instruments, Deerfield, IL) scanning electron microscope (SEM) was used to obtain SEM photomicrographs of Au-Pd coated specimens. Glass transition temperature (T<sub>g</sub>) determinations were conducted on a DuPont 9900 Computer/Thermal Analyzer-Model 943 Thermomechanical Analyzer (TMA) at a heating rate of 5°C/min.

The approach used to make solution property measurements has been previously reported.<sup>25</sup> Gel permeation chromatography (GPC) was performed on a Waters 150C GPC at 35°C in chloroform using a 10<sup>3</sup>/10<sup>4</sup>/10<sup>5</sup>/10<sup>6</sup>/Å Microstyragel™ HT column bank. The chromatograph was interfaced with a Waters

differential refractometer and a Viscotek (Viscotek Corp., Porter, TX) Model 150R Differential Viscometer (DV). A universal calibration curve was generated using Polymer Laboratories (Polymer Laboratories Inc., Amherst, MA) narrow dispersity polystyrene standards. GPC-DV analyses were conducted after samples had been in solution overnight.

## RESULTS AND DISCUSSION

The chemical structures of the experimental polymers are presented in Figures 1 and 2. The polymers are separated for convenience into fluorine-containing and silicon-containing. Fluorine-containing polymers flown in this experiment consisted of hexafluoroisopropylidene (6F)-containing polyimides, one poly(arylene ether) and one copoly(imide-arylene ether). The silicon-containing polymers consisted of four epoxy functionalized siloxanes (EFS) and one polyimide containing pendent siloxane groups (PISOX-1). The structures shown in Figure 2 for the EFS resins are prior to cure via UV radiation. These are one-part resins which contain ~1% of a photoinitiator catalyst (onium salt) and react via a cationic mechanism.<sup>24</sup>

Visual inspection of the two classes of exposed specimens revealed a marked difference in appearance. Fluorine-containing polymers were "frosted" or diffuse in appearance. In contrast, the silicon-containing polymers generally remained transparent and exhibited limited effects attributable to exposure. The two classes of polymer films were characterized by a number of analytical techniques. Thermo-mechanical analyses of the films showed no detectable change in  $T_g$ s of exposed films.

The initial weights, and weight losses of the films after LEO exposure are presented in Table 1. For comparative purposes, the weight loss data for FEP Teflon® on EOIM-III is included. The samples were either 1.0 in. or 0.5 in. in diameter and 0.001-0.003 in. thick. Consequently, the initial weights varied considerably. The fluorine-containing films exhibited higher weight losses after LEO exposure than either FEP Teflon® or the silicon-containing films. The weight losses for the fluorine-containing films were also higher with increasing exposure temperature, particularly when exposed at 200°C.

Most of the silicon-containing films were only exposed at 120°C due to limited space on the ambient exposure tray. They were not exposed at 200°C because of outgassing and subsequent contamination concerns. In general, silicon-containing films exhibited weight losses after 120°C exposure comparable to that exhibited by FEP Teflon® after ambient exposure (Table 1). The initial sample weights are included in Table 1. The ambient LEO exposed film from EFS-1 was brittle and broke apart during deintegration. Thus the weight loss could not be obtained. The ambient LEO exposed film from PISOX-1 exhibited a slight weight gain. This observation is reasonable since the silicon-containing polymers can gain weight by reacting with the AO to form silicate/silicon oxide. The overall trend exhibited by the weight loss data correlates well with observations from other analyses such as STM and XPS discussed later in this section.

Table 1. Weight Losses of Films after Exposure

Film Sample	Initial Weight, mg	Weight Loss, mg		
		Ambient Exposed	120°C Exposed	200°C Exposed
6F-PI-1	6.45 (120°C)	—	0.63	
	28.92 (200°C)			12.45
6F-PI-2	7.61 (ambient)	0.79		—
	8.84 (120°C)		0.92	
6F-PI-3	10.51 (ambient)	0.48		
	11.31 (120°C)		0.49	
	53.20 (200°C)			27.32
6F-PAE-1	3.76 (ambient)	0.42		—
	3.66 (120°C)		0.38	
6F-Co-PAE/PI-1	5.58 (ambient)	0.67		
	7.03 (120°C)		1.23	
	28.75 (200°C)			13.10
EFS-1	8.37 (120°C)	not available	0.36	—
EFS-2	31.27 (120°C)	—	0.01	—
EFS-3	30.48 (120°C)	—	0.21	—
EFS-4	43.55 (120°C)	—	0.11	—
PISOX-1	7.93 (ambient)	+0.30 (weight gain)		—
	24.69 (120°C)		0.01	
FEP Teflon®	15.60 (ambient)	0.03	—	—

### UV-VIS Spectroscopy

Films which acquired a "frosted" appearance with exposure exhibited significantly less UV-VIS transmission when compared to control films than did exposed films which did not appear "frosted". This phenomenon is illustrated in Figure 3 for each of the two classes of materials and is representative of spectra obtained for other fluorine and silicon-containing films. The decrease in transmission with exposure is attributed to light refraction and reflectance from surface roughness caused by AO erosion. The incorporation of fluorine into these type of materials was anticipated to reduce AO erosion since highly fluorinated vinyl polymers such as fluorinated ethylene propylene (FEP Teflon®) exhibit outstanding stability to the LEO environment.<sup>5,6,26</sup> There appeared to be a trend between higher exposure temperature and reduction of UV-VIS transmission (Figure 3). This observation correlates with the trend observed for higher weight loss with higher temperature exposure described earlier.

The silicon-containing films performed as expected, exhibiting no reduction in optical transmission by UV-VIS spectroscopy (Figure 4). The organically bound silicon (siloxane) was oxidized to inorganically bound silicon (silica/silicate) by atomic oxygen (see XPS section). The thin SiO<sub>x</sub> layer subsequently provided protection from further AO attack. This chemical transformation has been known and utilized in the microelectronics industry for some years.<sup>27</sup> This phenomenon has also been observed with other silicon-containing materials flown on several space flight exposure experiments.<sup>28-31</sup>

### Infrared Spectroscopy

Selected representative specimens were examined by FTIR spectroscopy. Since control and exposed films were too thick for high quality transmission spectra, somewhat lower quality diffuse reflectance spectra were obtained. Differences between control and exposed samples were difficult to assess visually. However, subtle differences could be detected by subtracting the two spectra.

The result of subtracting the exposed EFS-1 spectra from that of the control is presented in Figure 5. An upward inflection is indicative of more of a particular component in the control specimen. While differences in DR-FTIR subtraction spectra were generally not dramatic, several trends were noted.

DR-FTIR spectra of the fluorine-containing polyimides tended to exhibit 5-10 cm<sup>-1</sup> frequency shifts with exposure for the 1720, 1380 and 720 cm<sup>-1</sup> imide-related bands. While shifts were observed previously for other LEO-exposed polyimide films<sup>31,32</sup>, similar shifts have also been observed in our laboratory for thermally cured films which were not exposed in LEO. Thus, this feature remains uninterpreted. Most exposed silicon-containing polymers exhibited less aliphatic character with loss of methyl bands around 2970 cm<sup>-1</sup>. Film thinning was also observed with exposure as evidenced by an upward inflection in subtraction spectra of most specimens. The band around 3350 cm<sup>-1</sup> in the exposed film is presumably due to moisture absorption (hydration) of the SiO<sub>x</sub> surface which formed upon AO exposure.

### Solution Property Measurements

Only two sets of specimens were soluble before and after exposure. These two sets consisted of a fluorinated poly(arylene ether) (6F-PAE-1, Figure 1) exposed at ambient and 120°C and a fluorinated polyimide (6F-PI-1, Figure 1) exposed at 120 and 200°C, as well as the respective controls. Molecular weight analyses could only be conducted on these six films.

Number average ( $\overline{M}_n$ ), weight average ( $\overline{M}_w$ ), and Z average ( $\overline{M}_z$ ) molecular weight data along with the polydispersity ratio and intrinsic viscosities obtained by GPC-DV for the two soluble polymers are presented in Table 2. The fluorinated poly(arylene ether) appeared to undergo chain extension or possibly, slight crosslinking as evidenced by increases in ( $\overline{M}_n$ ), ( $\overline{M}_w$ ), and ( $\overline{M}_z$ ), and a 40% increase in hydrodynamic volume. These effects are attributable to UV degradation. This effect may be greater with elevated temperature exposure as the 120°C LEO exposed film exhibited larger increases in ( $\overline{M}_n$ ) and ( $\overline{M}_z$ ) compared to ambient LEO exposed and control films (Figure 6). The fluorinated polyimide appeared

to be stable to LEO exposure at all temperatures as no significant changes in the GPC data were evident. The apparent decrease in intrinsic viscosity with exposure for this material is not fully understood.

The molecular weight distributions for these two fluorinated polymers are presented in Figures 6 and 7. Distributions for the fluorine-containing poly(arylene ether) in Figure 6 show an increase in the high molecular weight component with exposure along with a corresponding decrease in the low molecular weight component. This observation is consistent with ( $\overline{M}_n$ ), ( $\overline{M}_w$ ), and ( $\overline{M}_z$ ) data given in Table 2. Molecular weight distributions for the fluorine-containing polyimide (Figure 7) show only minor differences with exposure.

Several polymers which received various LEO exposures have been characterized in previous studies. A polysulfone [i.e. poly(arylene ether)] film was found to undergo both chain scission and crosslinking after 10 months of LEO exposure onboard the Long Duration Exposure Facility (LDEF).<sup>33</sup> A sulfone-containing polyimide exhibited primarily crosslinking under identical exposure conditions on LDEF while a polyimide which contained isopropylidene and ether linkages (i.e. like polysulfone) exhibited no change in molecular weight.<sup>32</sup> A polysulfone film flown on a separate EOIM-III experiment also exhibited molecular level effects.<sup>34</sup> Thus, changes in various molecular weight parameters of soluble polymers resulting from LEO exposure can be readily characterized by GPC-DV. It appears that among aromatic polymers, not only is polymer family (i.e. imide vs. arylene ether) significant in regards to LEO stability, but the arrangement and type of connecting groups (i.e. ether, sulfone, carbonyl, etc.) is also important. However, our ability to predict how a particular polymer will respond to LEO exposure needs to be refined.

Table 2. Summary of GPC Results

Sample ID	( $\overline{M}_n$ ) g/mole	( $\overline{M}_w$ ) g/mole	( $\overline{M}_z$ ) g/mole	Polydispersity	Intrinsic Viscosity, dL/g
<b>6F-PAE-1</b>					
Control	9408	35,930	68,600	3.81	0.459
Exposed (Ambient)	13,910	44,740	133,800	3.21	0.436
Exposed (120°C)	13,750	67,870	494,000	4.94	0.429
<b>6F-PI-1</b>					
Control	38,330	129,900	273,200	3.38	0.699
Exposed (120°C)	34,530	143,600	310,000	4.16	0.608
Exposed (200°C)	44,040	145,100	313,200	3.29	0.632

### Surface Analysis

As mentioned earlier, LEO exposed fluorine-containing films exhibited a "frosted" appearance both visually and by optical microscopy. Further detailed data from STM and SEM analyses are shown in Figures 8 and 9, respectively. The fluorine-containing films appeared heavily eroded and shared identical marble-like erosion patterns unique in comparison to similar polymers flown of LDEF which exhibited an egg-crate-like erosion surface.<sup>35</sup>

The silicon-containing films exhibited no discernible differences between exposed and control samples by optical microscopy. However, analyses by SEM and STM indicated that some surface erosion did occur. The STM line plot of EFS-4 is presented in Figure 10. Note that when comparing the erosion depths in Figures 8 and 10 that the depth profile scales are different. STM spectra of the LEO exposed film shows the beginnings of the egg-crate-like pattern seen previously in AO exposed polymer films.<sup>35</sup> Presumably, initial AO erosion occurs until a sufficient layer of SiO<sub>x</sub> is formed from the reaction of the oxygen atoms with the silicon.

Table 3. XPS Results of EFS-1

Photopeak	Control	LEO upside ambient exposed	LEO downside ambient exposed	LEO upside 120°C exposed	LEO downside 120°C exposed
<b>C1s</b>					
Binding Energy ,eV	284.6	284.6	284.6	284.6	284.6
Atomic	65.9	38.7	61.7	18.3	73.6
Concentration , %					
<b>O1s</b>					
Binding Energy ,eV	532.1	532.8	532.6	533.1	532.0
Atomic	19.5	38.5	27.1	53.1	17.9
Concentration , %					
<b>Si2p</b>					
Binding Energy ,eV	101.8	103.7	101.9	103.2	101.4
Atomic	14.6	21.4	9.1	28.2	7.0
Concentration , %					
<b>N1s</b>					
Binding Energy ,eV	—	399.0	399.9	399.5	399.8
Atomic	—	1.4	2.2	0.5	1.5
Concentration , %					

### X-Ray Photoelectron Spectroscopy (XPS)

X-ray photoelectron spectroscopy was performed at Virginia Polytechnic Institute and State University under NASA Langley Grant NAG1-1186. Representative samples of control and exposed fluorine and silicon-containing films were analyzed using XPS. The fluorine-containing polyimide (6F-PI-2) for the most part indicated little difference in the control sample and either side of the exposed samples. However, there was some difference in the atomic concentration of the fluorine on both LEO exposure sides of the ambient and 120°C exposed films. Silicon contamination was identified on both control (~2%) and exposed (1-3.8%) samples.

XPS data for EFS-1 exposed at both ambient and 120°C is presented in Table 3. There was a clear difference in XPS data from upside versus downside LEO exposed films. The upside LEO exposed films exhibited dramatic changes in surface chemistry. The downside of the films did not receive AO or UV exposure and consequently exhibited no changes in surface chemistry (Table 3). The silicon was oxidized to silicate/silicon oxide as evidenced by the increases in binding energy of the Si2p electrons on the LEO upside

Table 4. XPS Results of PISOX-1

Photopeak	Control	LEO upside ambient exposed	LEO downside ambient exposed	LEO upside 120°C exposed	LEO downside 120°C exposed
<b>C1s</b>					
Binding Energy ,eV	284.6	284.6	284.6	284.6	284.6
Atomic Concentration , %	69.2	26.7	58.7	29.3	68.7
<b>O1s</b>					
Binding Energy ,eV	532.1	532.8	532.6	533.1	532.0
Atomic Concentration , %	19.1	46.0	27.8	45.4	21.9
<b>Si2p</b>					
Binding Energy ,eV	101.6	103.1	102.4	103.4	101.6
Atomic Concentration , %	9.3	25.7	11.5	24.2	5.5
<b>N1s</b>					
Binding Energy ,eV	400.2	399.9	399.7	399.8	400.1
Atomic Concentration , %	2.4	0.9	1.9	1.1	3.9

exposed films. In addition, the atomic concentration of Si on the LEO upside exposed films increased from 14.6% (control) to 21.4 and 28.2%, respectively for the ambient and 120°C exposures. The oxygen 1s electron binding energies showed slight increases as did the atomic concentration of oxygen for the LEO exposed side of the films (Table 3). There were differences in the XPS data of the ambient LEO upside exposures compared to those of the 120°C exposures. The atomic concentrations for silicon and oxygen were higher for the 120°C exposed films. The XPS data for EFS-2 exhibited the same general trends as those described for EFS-1.

The polyimide containing pendent siloxane groups (PISOX-1) exhibited similar behavior in regards to the increases in binding energies of the silicon and oxygen electrons and atomic concentrations of the LEO exposed (upside) films (Table 4). These increases in binding energies and atomic concentrations are consistent with AO induced organo-silicon to silicate/silicon oxide chemical transformations. After exposure, the silicon-containing materials typically exhibited a ratio of silicon:oxygen of approximately 1:2. There appeared to be a trend between ambient exposed and elevated temperature exposed specimens of silicon-containing polymers in that the atomic concentration of silicon and oxygen were higher for the samples exposed at elevated temperature. Similar behavior, with respect to organo-silicon to inorgano-silicon chemical changes, has been observed for copoly(imide-siloxane) flown on LDEF.<sup>28-31</sup> The silicon and oxygen in these materials exhibited increases in binding energies and relative concentrations that were attributed to SiO<sub>x</sub> formation as a result of the AO exposure. In addition, these materials exhibited lower erosion rates than other non-silicon containing organic polymers.

## SUMMARY

A series of experimental fluorine and silicon-containing polymer films were exposed to LEO at several different temperatures aboard the STS-46 materials exposure flight experiment EOIM-III. The fluorine-containing materials were dramatically affected by relatively short term AO and UV exposure. They exhibited "frosting" with corresponding reductions in optical transmission as a result of AO exposure. The 6F-PAE-1 exhibited changes in molecular weight distribution characteristic of UV induced degradation while the 6F-PI-1 exhibited little, if any changes. The weight loss and UV-VIS data suggest that samples exposed at elevated temperature in LEO exhibited more pronounced AO effects (i.e. higher weight loss and greater reduction in optical transparency) compared to ambient LEO exposed samples. The fluorine-containing films exhibited a unique erosion pattern different than those observed on films flown on LDEF. Fluorine-containing materials of this type obviously would need to be protected from AO exposure.

The silicon-containing polymers exhibited little effects of the LEO exposure. The films remained clear with no significant reductions in optical transparency. Conversion of the organo-silicon to silicate/silicon oxide was evident from the XPS data and formation of this SiO<sub>x</sub> surface layer undoubtedly

protected the underlying material from further erosion. Initial erosion due to AO was observed. This is necessary to allow sufficient reaction of the atomic oxygen with the silicon to form an in-situ SiO<sub>x</sub> protective coating. Further work will focus on the effects of longer duration ground based exposures of these materials.

## REFERENCES

1. P. N. Peters, R. C. Linton and E. R. Miller, *J. Geophys. Res. Lett.*, 10, 569 (1983).
2. D. E. Bowles and D. R. Tenney, *SAMPE J.*, 23(3), 49 (1987).
3. W. S. Slemph, B. Santos-Mason, G. F. Sykes Jr. and W. G. Witte Jr., *AO Effect Measurements for Shuttle Missions STS-8 and 41-G, Vol 1, Sec 5, 1* (1985).
4. *LDEF-69 Months in Space. First Post Retrieval Symposium. NASA Conference Publication 3134 Part 2*, A. Levine Ed., 1991.
5. L. J. Leger, J. T. Visentine and B. Santos-Mason, *SAMPE Quaterly*, 18(2), 48 (1987).
6. A. E. Stiegman, D. E. Brinza, M. S. Anderson, T. K. Minton, G. E. Laue and R. H. Liang, *Jet Propulsion Laboratory Publication 91-10*, May 1991.
7. B. A. Banks, M. J. Mistich, S. K. Rutledge and H. K. Nahra, *Proc. 18<sup>th</sup> IEEE Photovoltaic Specialists Conf.*, 1985.
8. L. J. Leger, I. K. Spikes, J. F. Kuminecz, T. J. Ballentine and J. T. Visentine, *STS Flight 5, LEO Effects Experiment*, AIAA-83-2631-CP (1983).
9. K. A. Smith, *Evaluation of Oxygen Interactions with Materials (EOIM), STS-8 AO Effects*, AIAA-85-7021 (1985).
10. S. Packrisamy, D. Schwam, and M. Litt, *Polym. Prepr.*, 34(2), 197 (1993).
11. J. T. Visentine, L. J. Leger, J. F. Kuminecz and I. K. Spiker, *AIAA-85-0415*, AIAA 23rd Aerospace Conf., Jan. (1985).
12. C. A. Arnold, J. D. Summers, Y. P. Chen, R. H. Bott, D. H. Chen and J. E. McGrath, *Polymer*, 30(6), 986 (1989).
13. C. A. Arnold, J. D. Summers, Y. P. Chen, T. H. Yoon, B. E. McGrath, D. Chen and J. E. McGrath, in *Polyimides: Materials, Chemistry and Characterization*, C. Feger, Ed., Elsevier Science Publishers B. V., Amsterdam, 1989, pp. 69-89.
14. C. A. Arnold, D. H. Chen, Y. P. Chen, R. O. Waldbauer, Jr., M. E. Rogers and J. E. McGrath, *High Perf. Polymers*, 2(2), 83 (1990).
15. J. W. Connell, D. C. Working, T. L. St. Clair and P. M. Hergenrother, in *Polyimides: Materials, Chemistry, and Characterization*, C. Feger, Ed., Technomic Pub. Co., Lancaster, PA, 1992, pp. 152-164.
16. J. W. Connell, J. G. Smith, Jr. and P. M. Hergenrother, *J. Fire Sci.*, 11(2), 137 (1993).

17. P. R. Young and W. S. Slempp, LDEF Materials Workshop '91, *NASA Conf. Pub. 3162 Part 1*, 376-378 (1991).
18. J. Kulig, G. Jefferis and M. Litt, *Polym. Matl. Sci. Eng.*, 61, 219 (1989).
19. A. K. St. Clair, T. L. St. Clair and W. S. Slempp, in *Recent Advances in Polyimide Science and Technology*, W. D. Weber and M. R. Gupta, Eds., Soc. Plast. Eng., Poughkeepsie, NY, 1987, pp. 16-36.
20. J. W. Connell, E. J. Siochi and C. I. Croall, *High Perf. Polymers*, 5, 1 (1993).
21. M. K. Gerber, J. R. Pratt, A. K. St. Clair and T. L. St. Clair, *Polym. Prepr.*, 31(1) 340 (1990). F. W. Harris, S. L.-C. Hsu and C. C. Tso, *ibid.*, 342 (1990). R. A. Buchanan, R. F. Mundhenke and H. C. Lin, *ibid.*, 32(2), 193 (1991).
22. R. N. Johnson, A. G. Farnham, F. A. Clendinning, W. F. Hale and C. N. Merriam, *J. Polym. Sci.*, 5, 2375 (1967).
23. B. J. Jensen and S. J. Havens, *Polym. Prepr.*, 33(1), 1084 (1992).
24. J. V. Crivello and J. L. Lee, *J. Polym. Sci. Polym. Chem. Ed.*, 28 479 (1990).
25. P. R. Young, J. R. J. Davis and A. C. Chang, *Soc. Adv. Matls. and Proc. Eng. Ser.*, 34(2), 1450 (1989).
26. P. R. Young, W. S. Slempp, *NASA Technical Memorandum 104096*, (Dec. 1991).
27. N. J. Chou, C. H. Tang, J. Paraszczak and E. Babich, *Appl. Phys. Lett.*, 46(1), 31 (1985).
28. P. R. Young, W. S. Slempp, W. G. Witte and J. Y. Shen, *Soc. Adv. Matls. and Proc. Eng. Ser.*, 36(1), 403 (1991).
29. M. J. Meshishnek, W. K. Stuckey, J. S. Evangelsides, L. A. Feldman, R. V. Peterson, G. S. Arnold and D. R. Peplinski, *NASA Technical Memorandum 100459, Vol. II, Sec. 5-1 to 5-33* (1988).
30. W. S. Slempp, B. Santos-Mason, G. F. Sykes and W. G. Witte, *ibid.*, Vol. I, Sec. 5-1 to 5-15 (1988).
31. P. R. Young, W. S. Slempp and C. R. Gautreaux, *Soc. Adv. Matls. and Proc. Eng. Ser.*, 37(1), 159 (1992).
32. P. R. Young, A. K. St. Clair and W. S. Slempp, *Soc. Adv. Matls. and Proc. Eng. Ser.*, 38(1), 664 (1993).
33. P. R. Young, W. S. Slempp, E. J. Siochi and J. R. J. Davis, *SAMPE Tech. Conf. Proc.*, 24, T174 (1992).
34. P. R. Young, W. S. Slempp and E. J. Siochi, *Soc. Adv. Matls. and Proc. Eng. Ser.*, 39, 2243 (1994).
35. C. R. Kalil and P. R. Young, *Soc. Adv. Matls. and Proc. Eng. Ser.*, 39(1), 445 (1993).

The use of trade names of manufacturers does not constitute an official endorsement of such products or manufacturers, either expressed or implied, by the National Aeronautics and Space Administration.

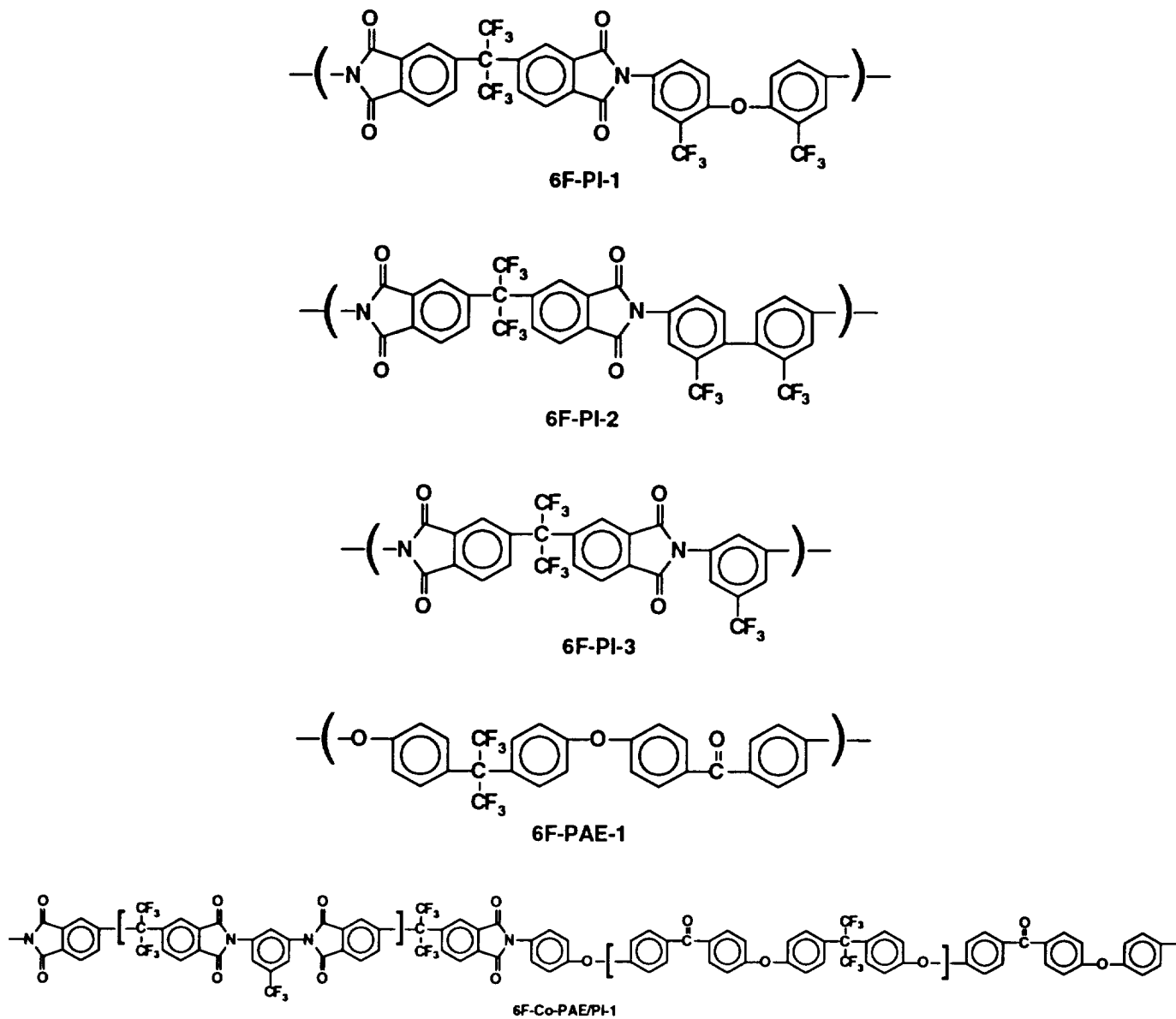


Figure 1. Chemical structures of fluorine-containing polymers.

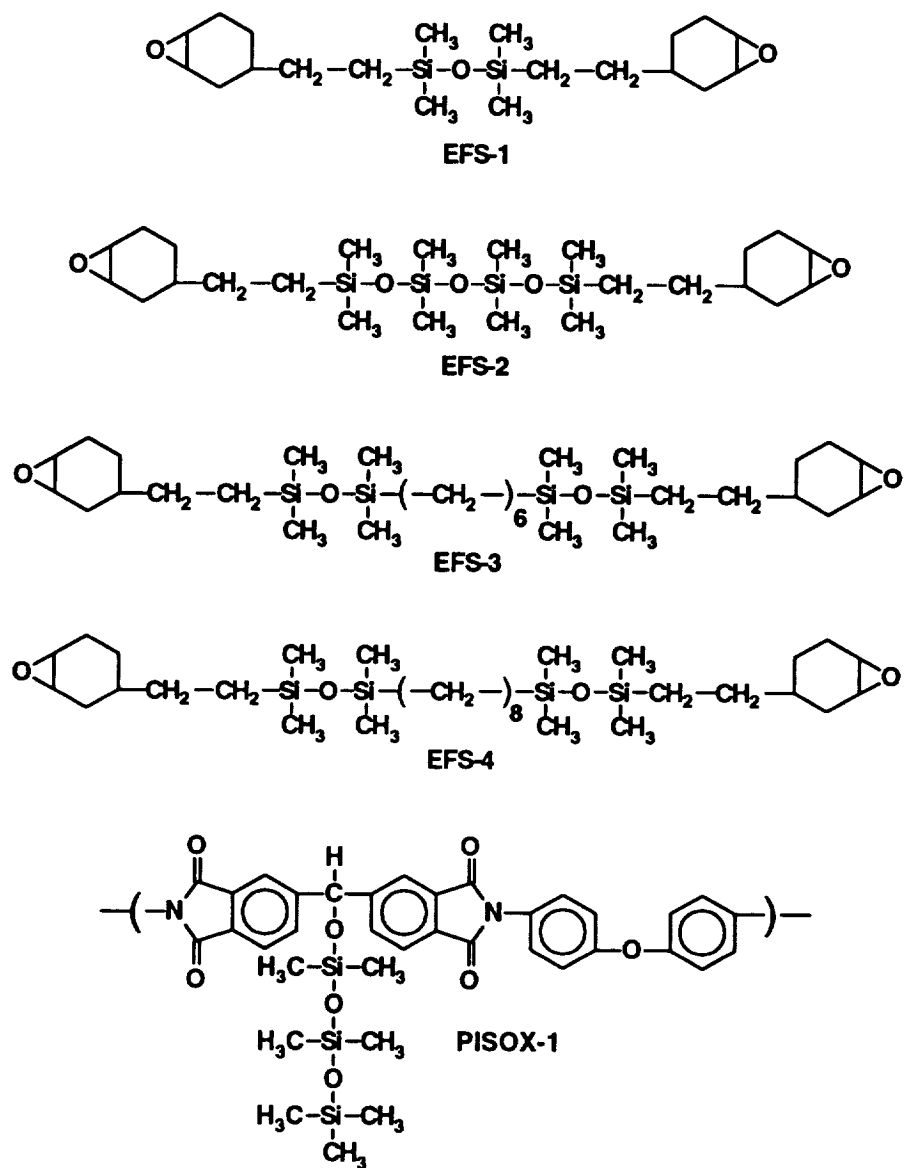


Figure 2. Chemical structures of silicon-containing polymers, the structures given for the EFS compounds are prior to curing with a UV source.

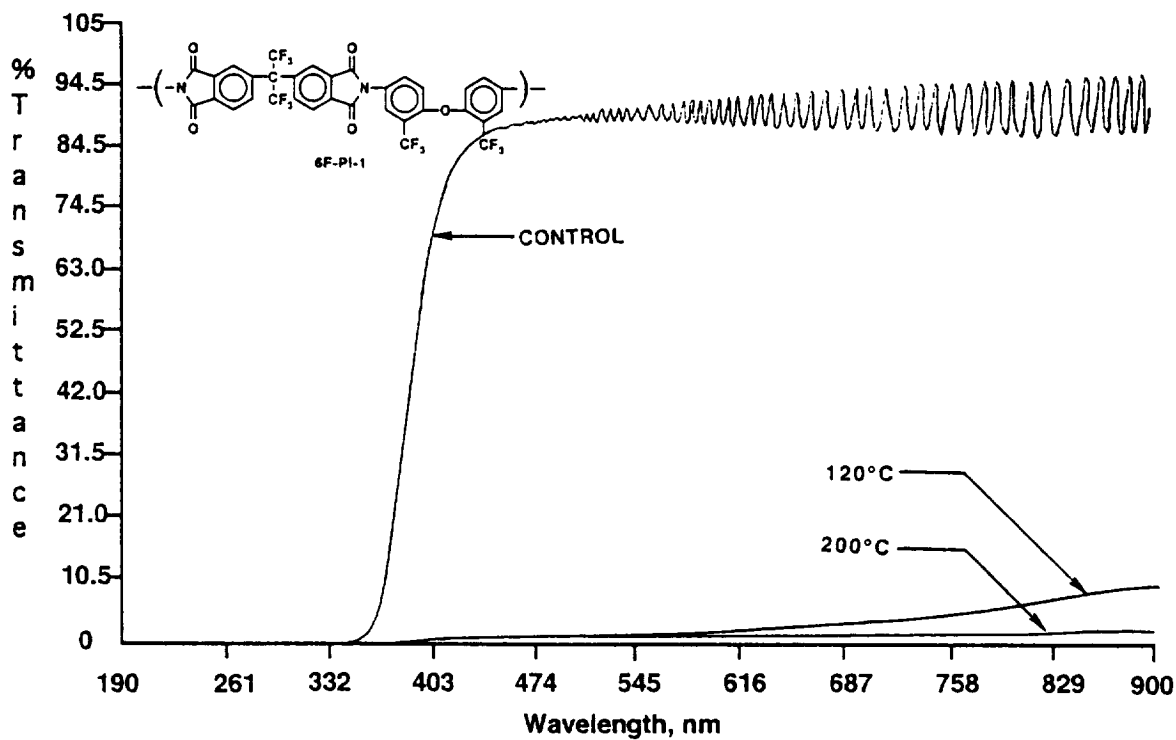


Figure 3. UV-VIS overlay spectra of fluorine-containing polyimide (6F-PI-1) before and after LEO exposure.

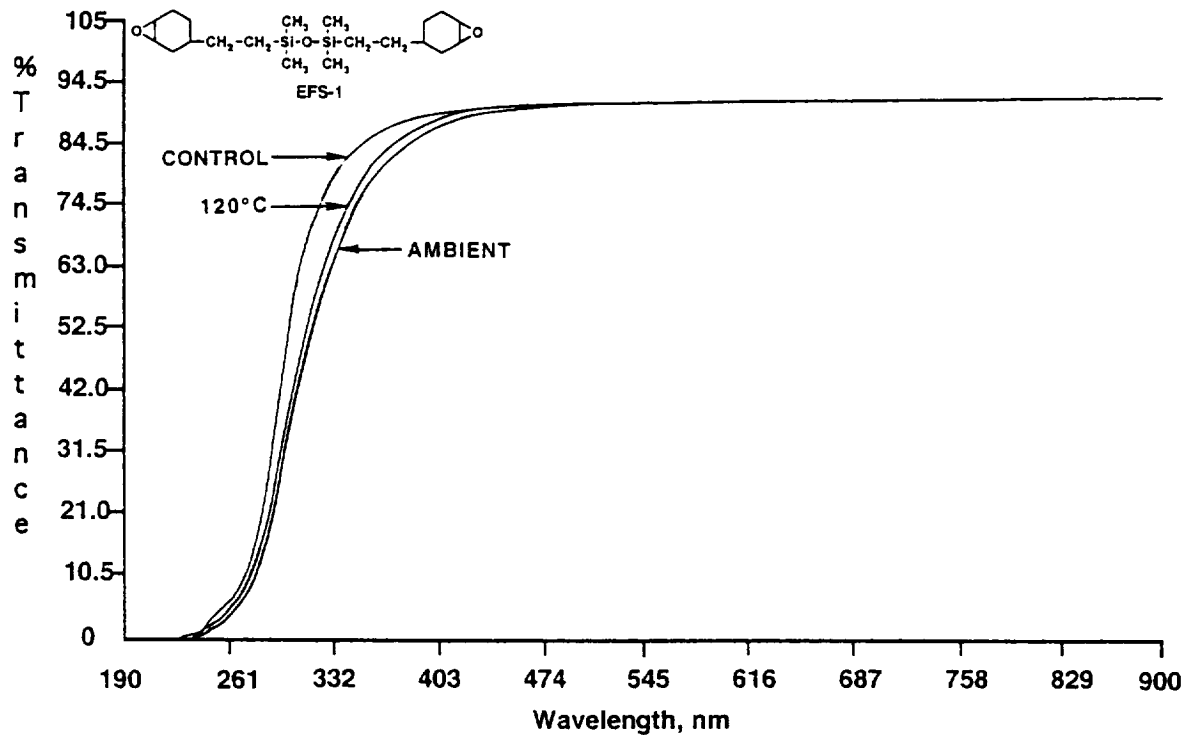


Figure 4. UV-VIS overlay spectra of silicon-containing epoxy (EFS-1) before and after LEO exposure.

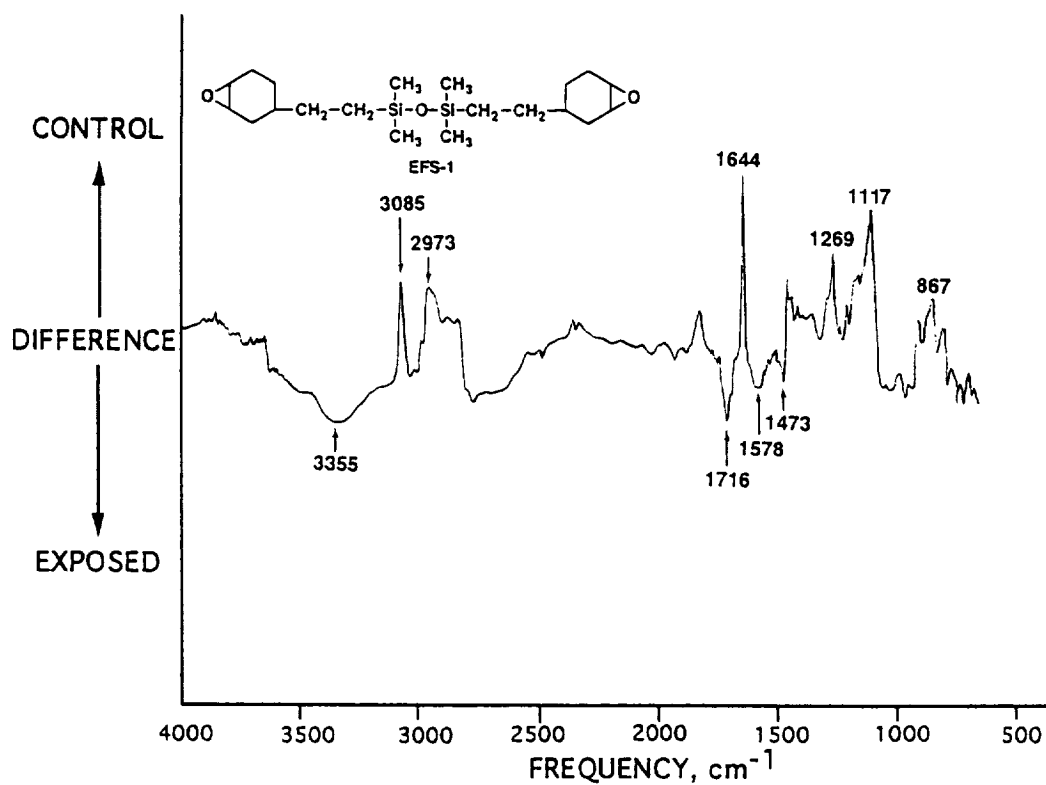


Figure 5. DR-FTIR subtraction spectrum of silicon-containing epoxy (EFS-1) before and after LEO exposure.

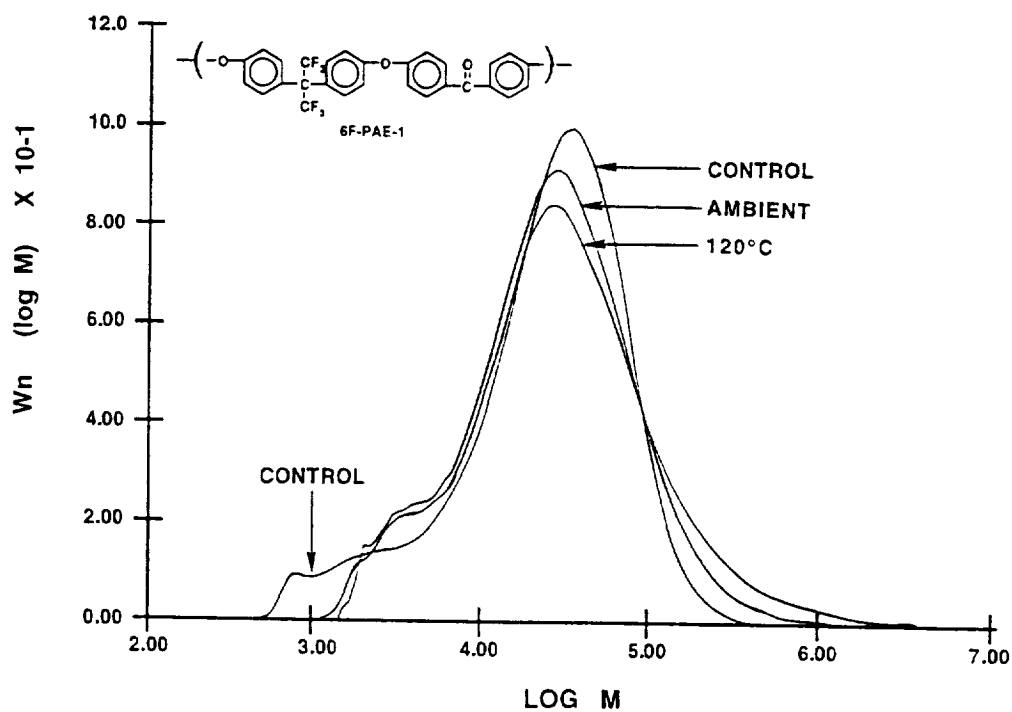


Figure 6. Overlay of molecular weight distributions of fluorine-containing poly(arylene ether), 6F-PAE-1, before and after LEO exposure.

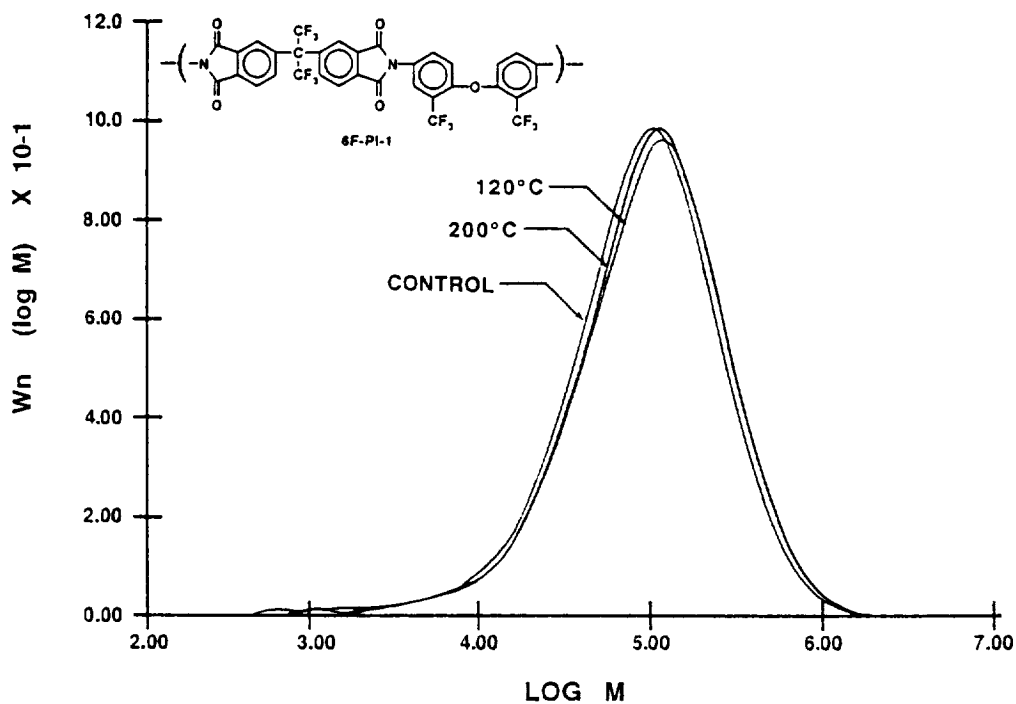


Figure 7. Overlay of molecular weight distributions of fluorine-containing polyimide, 6F-PI-1, before and after LEO exposure.

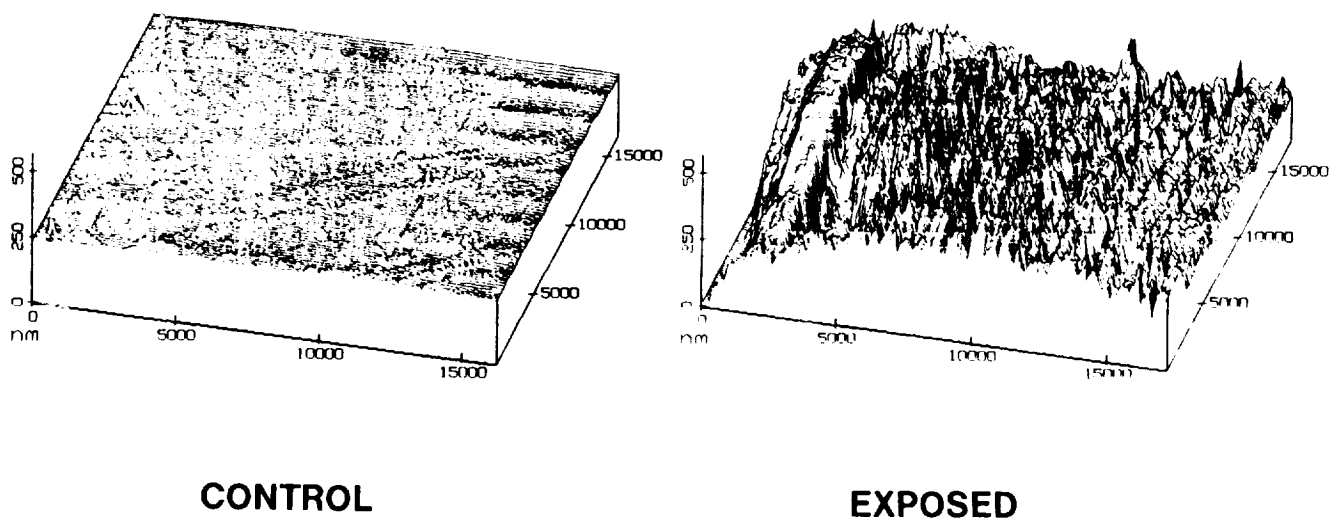
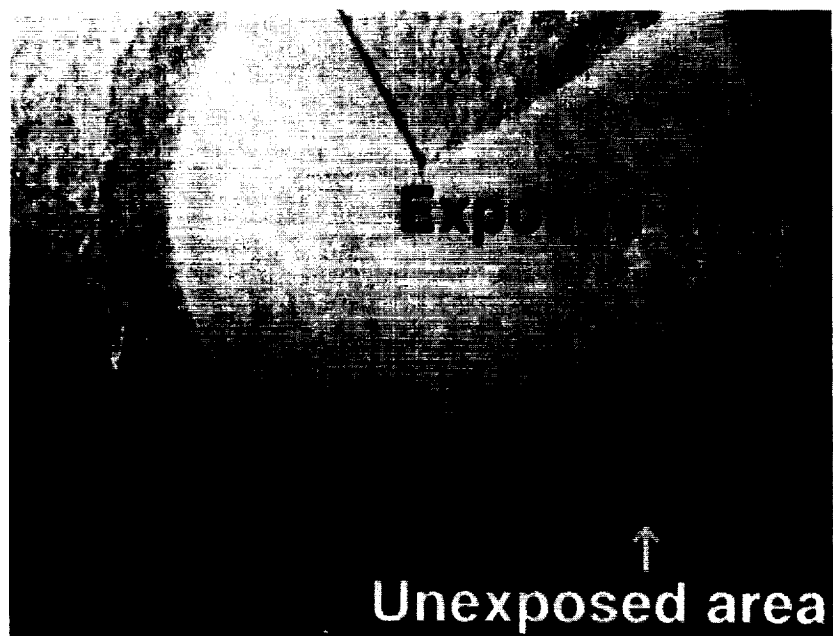
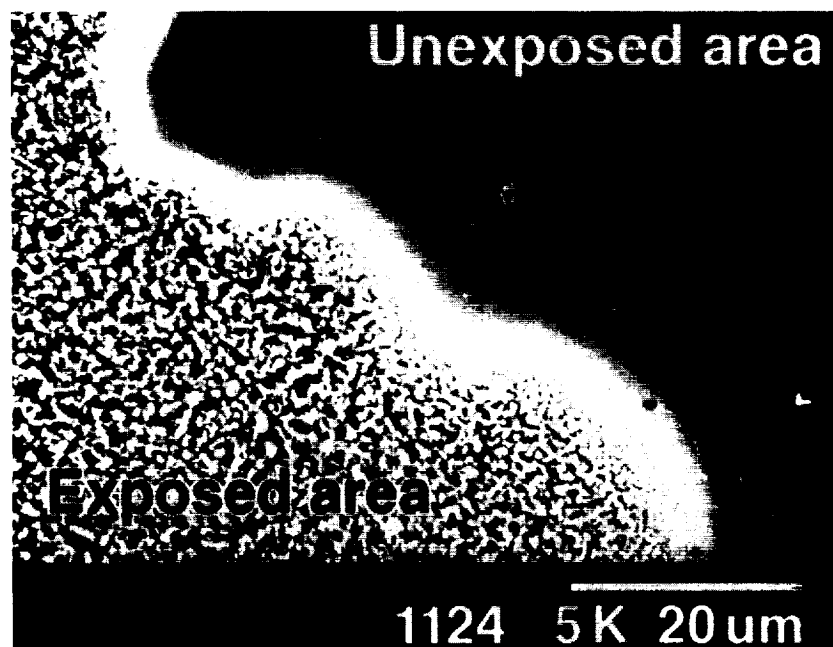


Figure 8. STM of fluorine-containing poly(arylene ether), 6F-PAE-1, before and after LEO exposure.

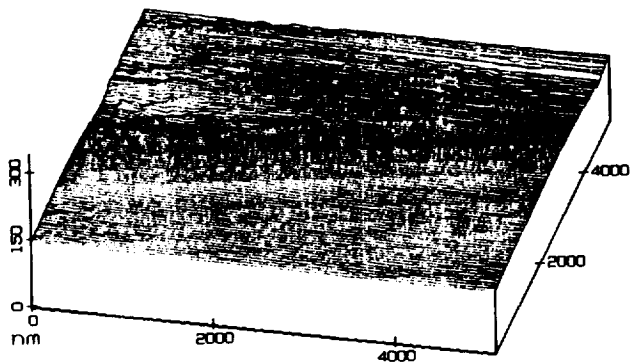


**Optical microscopy (8X)**

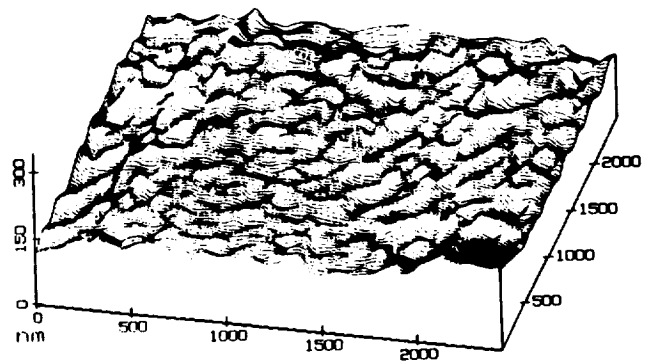


**Scanning electron microscopy**

Figure 9. Photomicrographs of fluorine-containing poly(arylene ether), 6F-PAE-1, before and after LEO exposure.



**CONTROL**



**EXPOSED**

Figure 10. STM of silicon-containing epoxy (EFS-4) before and after LEO exposure.

